

The Identification of Residues That Control Signal Peptidase Cleavage Fidelity and Substrate Specificity*

Received for publication, November 17, 2004

Published, JBC Papers in Press, December 14, 2004, DOI 10.1074/jbc.M413019200

Andrew Karla‡§, Mark O. Lively¶, Mark Paetzel||**, and Ross Dalbey‡ ||‡

From the ‡Department of Chemistry, The Ohio State University, Columbus, Ohio 43210, the ¶Department of Biochemistry, Wake Forest University School of Medicine, Winston-Salem, North Carolina 27157, and the ||Department of Molecular Biology and Biochemistry, Simon Fraser University, Burnaby, British Columbia V5A 1S6, Canada

Signal peptidase, which removes signal peptides from preproteins, has a substrate specificity for small uncharged residues at -1 (P1) and small or larger aliphatic residues at the -3 (P3) position. Structures of the catalytic domain with a 5S-penem inhibitor and a lipopeptide inhibitor reveal candidate residues that make up the S1 and S3 pockets that bind the P1 and P3 specificity residues of the preprotein substrate. We have used site-directed mutagenesis, mass spectrometric analysis, and *in vivo* and *in vitro* activity assays as well as molecular modeling to examine the importance of the substrate pocket residues. Generally, we find that the S1 and S3 binding sites can tolerate changes that are expected to increase or decrease the size of the pocket without large effects on activity. One residue that contributes to the high fidelity of cleavage of signal peptidase is the Ile-144 residue. Changes of the Ile-144 residue to cysteine result in cleavage at multiple sites, as determined by mass spectrometry and Edman sequencing analysis. In addition, we find that signal peptidase is able to cleave after phenylalanine at the -1 residue in a double mutant in which both Ile-86 and Ile-144 were changed to an alanine. Also, alteration of the Ile-144 and Ile-86 residues to the corresponding residues found in the homologous Imp1 protease changes the specificity to promote cleavage following a -1 Asn residue. This work shows that Ile-144 and Ile-86 contribute to the signal peptidase substrate specificity and that Ile-144 is important for the accuracy of the cleavage reaction.

In all living cells, proteins that are exported to the cell surface are synthesized with an N-terminal, cleavable signal peptide. The signal peptides are then proteolytically removed by a type I signal peptidase (SPase)¹ that has its catalytic domain on the trans side of the membrane.

SPases have been identified and characterized in a wide

variety of Gram-negative and Gram-positive bacteria, mitochondria, and the endoplasmic reticulum (for reviews, see Refs. 1 and 2). Except for the SPase found in the endoplasmic reticulum, the SPases are proteases that use a serine-lysine catalytic dyad mechanism (3–9). The active site serine residue, Ser-90 in *Escherichia coli* SPase, is conserved in the homologous subunit within the endoplasmic reticulum signal peptidase complex. However, it differs from the bacterial and organelar SPases by the substitution of a histidine in place of the catalytic lysine. The endoplasmic reticulum signal peptidase uses either a serine-histidine dyad mechanism or the classical serine-histidine-aspartic acid triad mechanism (4).

The crystal structure of the *E. coli* signal peptidase with covalently attached inhibitor proved that SPase is a serine protease and is consistent with Lys-145 being involved in the activation of the nucleophilic Ser-90 (10). The structure provided a picture of how SPase can bind and cleave signal peptides from exported proteins. Fig. 1 shows a structural model of the *E. coli* SPase (shown in a light gray ribbon diagram) with a theoretical model of a signal peptide (yellow) docked into its substrate binding sites (displayed as a molecular surface, green, red, cyan). One of the striking features of the protein structure is a large hydrophobic patch comprised of an antiparallel β -strand domain (residues 81–85, 99–105, 292–307, and 312–314) that we believe allows the catalytic domain to interact with the membrane during catalysis. Fig. 1A shows the proposed orientation of SPase relative to the membrane surface with the hydrophobic domain (indicated in yellow) of the signal peptide extending downwards into the lipid bilayer.

In both prokaryotic and eukaryotic organisms, SPase exhibits similar substrate requirements. With the exception of mitochondrial Imp1, type 1 SPase specifically recognizes substrates with small amino acid residues at the -1 (P1) position or small uncharged residues at the -3 (P3) position of the signal peptide relative to the cleavage site (11–14). The identity of determinants within SPase that control cleavage of the substrate at the correct site and not at other nearby potential sites remains unknown. The substrate specificity determinants within SPase that allow it to cleave signal peptides following the -3 , -1 rule are also undefined. One clue comes from the structure. The structure of *E. coli* SPase with a bound inhibitor indicates that nonpolar atoms from the residues Ile-86, Pro-87, Ser-88, Gly-89, Ser-90, Met-91, Leu-95, Tyr-143, Ile-144, and Lys-145 form the S1 pocket. In addition, modeling studies suggest that nonpolar atoms from the residues Phe-84, Ile-86, Ile-101, Val-132, Asp-142, and Ile-144 comprise the S3 pocket (10). The residues Ile-144 and Ile-86 (colored red in Fig. 1) bridge the S1 and S3 binding pockets.

As a first step to identify residues that control cleavage fidelity, and substrate specificity, we mutated residues in the *E. coli* SPase substrate binding site and examined the effects of

* This work was supported by in part by National Science Foundation Grant MCB-0316670 (to R. E. D.) and by operating grants from the Canadian Institute of Health Research (to M. P.) and the National Science and Engineering Research Council of Canada (to M. P.). The costs of publication of this article were defrayed in part by the payment of page charges. This article must therefore be hereby marked "advertisement" in accordance with 18 U.S.C. Section 1734 solely to indicate this fact.

§ Supported by the National Institutes of Health Chemistry-Biology Interface Training Program Grant T32GM08512.

¶ Recipient of a scholar award recipient from the Michael Smith Foundation for Health Research.

** To whom correspondence should be addressed. Tel.: 614-292-2384; Fax: 614-292-1532; E-mail: dalbey@chemistry.ohio-state.edu.

1 The abbreviations used are: SPase, signal peptidase; MALDI-TOF, matrix-assisted laser desorption/ionization time-of-flight; PONA, proOmpA nuclease A; WT, wild type.

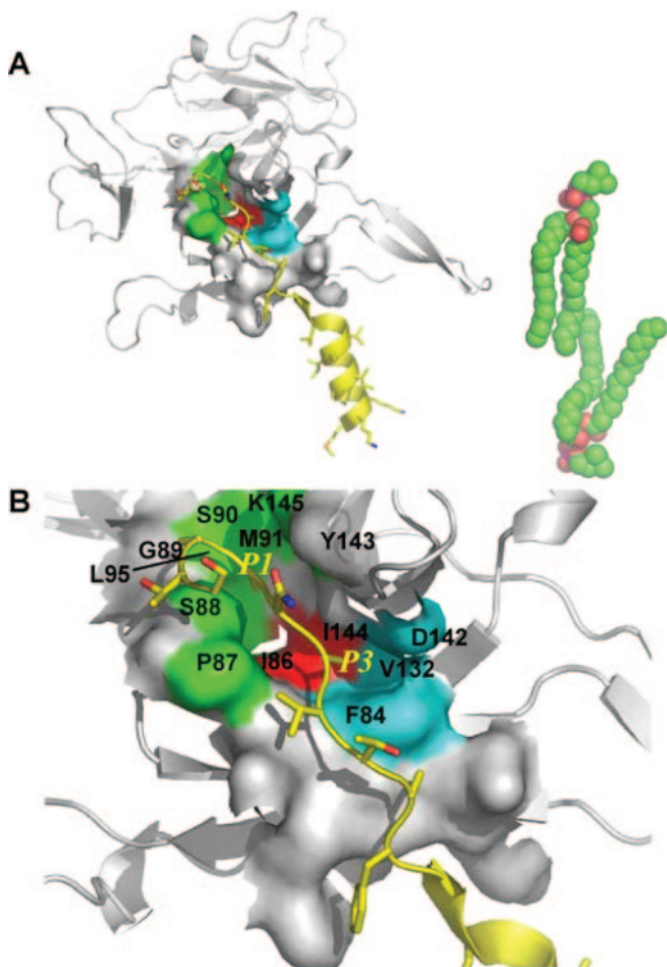


FIG. 1. A model of signal peptidase in complex with the signal peptide of the substrate PONA. *A*, a ribbon diagram of signal peptidase is rendered in light grey. The molecular surface is shown for those residues of signal peptidase within 5 Å of the PONA signal peptide (yellow). Two phospholipids molecules are shown in van der Waals spheres (green and red) to give perspective and orientation relative to the membrane. *B*, a close-up view of the signal peptidase substrate binding pockets. The molecular surface is colored green for those signal peptidase residues contributing side chain atoms to the S1 pocket. The molecular surface is colored cyan for those residues contributing side chain atoms to the S3 pocket. The molecular surface is colored red for the residues isoleucine 86 and isoleucine 144. The surface main chain atoms and surface atoms not part of the S1 or S3 binding pockets are colored white. The signal peptidase residues are labeled in black, and the P1 alanine and P3 alanine of the PONA signal peptide are labeled in yellow.

those changes on the cleavage of various substrates. We found that substitution of SPase Ile-144 by a cysteine residue results in cleavage of the proOmpA nuclease A substrate at multiple sites. Cleavage at multiple sites is in contrast to the action of wild-type SPase, which cleaves exclusively at the correct site. The cleavage at multiple sites suggests that Ile-144 contributes to the high fidelity of cleavage by SPase enzymes. In addition, we found that mutation of Ile-86 and Ile-144 to alanine residues changes the specificity of the enzyme, allowing it to cleave after a (-1) Phe residue. Lastly, substitution of Ile-144 and Ile-86 residues by the homologous residues found in the Imp1 protease changes the specificity by promoting cleavage following a (-1) Asn residue. Taken together, the results demonstrate that Ile-144 and Ile-86 play important roles in substrate specificity and cleavage fidelity.

EXPERIMENTAL PROCEDURES

Bacterial Strains and Plasmids—*E. coli* strains BL21(DE3), BLR(DE3), and DH5 α were from our collection. *E. coli* IT41, a temper-

ature-sensitive SPase I strain, was obtained from Dr. Yoshikazu Nakamura (15). The IT41 cell line was modified by incorporation of the T7 RNA polymerase gene using λ DE3 prophage supplied in the λ DE3 lysogenization kit (Novagen) to produce IT41(DE3). Lysogens successfully expressing the T7 RNA polymerase were verified using the included T7 tester phage in addition to verifying temperature-sensitive growth. The pET 23b vector, which contains isopropyl-1-thio- β -D-galactopyranoside-inducible SPase with a His₆ tag, was described previously (16). The pONF1 vector overexpressing proOmpA nuclease A was described in Ref. 17. This nuclease A substrate has a six-histidine sequence at codons 2–7 (18).

DNA Methods—The QuikChange mutagenesis method (Stratagene Inc.) was used to make oligonucleotide-directed mutations within the SPase and proOmpA nuclease A proteins. Mutations were verified by gene sequencing. The calcium chloride and electroporation methods were used for DNA transformation into *E. coli* strain, DH5 α .

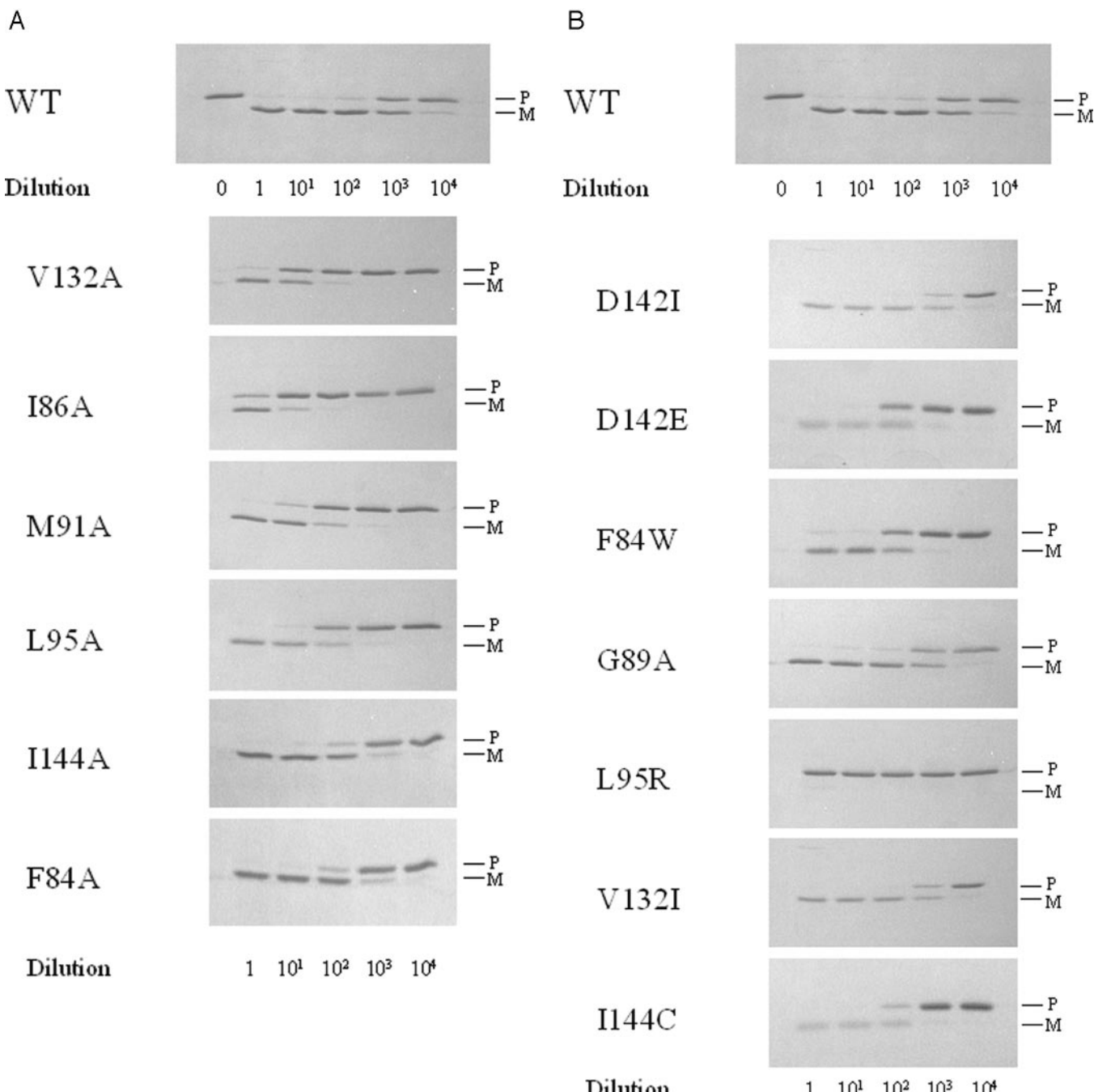
Purification of Signal Peptidase and proOmpA Nuclease A—BL21(DE3) cells containing His₆-tagged SPase encoded by the pET23b vector were used for overexpression of SPase. SPase was expressed and purified using ion exchange and nickel affinity chromatography, as described by Ref. 16. ProOmpA nuclease A containing a His₆ tag was purified over a Ni²⁺-nitrilotriacetic acid-agarose (Qiagen, Inc.) column, as described in Ref. 18, with modifications to utilize denaturing conditions. Following ammonium sulfate precipitation, proteins were dissolved in 6 M guanidine buffer and loaded on 1-ml bed volume of nickel-nitrilotriacetic acid resin. Resin was washed with 8 M urea buffer (pH 8.0) to remove guanidine, and elution of bound protein was accomplished using 8 M urea buffers of reducing pH (pH 6.3, 5.9, 4.5). Following elution, proteins were assayed for purity using 17% SDS-PAGE, and selected fractions were refolded slowly by dialyzing against increasing volumes of 25 mM HEPES (pH 7.5) with 1% Triton X-100 utilizing a total of 4 liters of buffer.

In Vitro and In Vivo Assay of Signal Peptidase Cleavage—The *in vitro* activity of wild-type and mutant SPases was determined using various proOmpA nuclease A substrates. Cleavage of the substrate was performed at different dilutions of SPase, as described (16). To determine the activity of SPase *in vivo*, we used the temperature-sensitive IT41(DE3) strain. The IT41(DE3) strain was modified from the original strain by introducing the T7 RNA polymerase gene, allowing expression of the pET 23b encoded SPases. The procedure for measuring *in vivo* activity of the SPase mutants is the same as that described by Ref. 16. Single colony transformants of IT41(DE3) were transferred into M9+glucose media and grown to a density of ~0.3 A₆₀₀. The cells were then shifted to 42 °C and incubated for an additional 1.5 h. The cells were pulsed with [³⁵S]methionine for 10 s and then chased with non-radioactive methionine for the indicated times.

Complementation of the Growth Defect—The processing of proOmpA was assayed in the temperature-sensitive SPase strain, IT41(DE3). All medium used to culture IT41(DE3) were prepared with a low salt concentration (2.5 g NaCl/liter). Competent cells of IT41(DE3) were prepared using the CaCl₂ method and transformed with a plasmid expressing the SPase mutant to be studied. The transformed IT41(DE3) cells were plated on solid medium with 100 μ g/ml ampicillin and grown at 30 °C until colonies reached 1–2 mm in size. Single transformants were selected and resuspended in fresh medium and streaked in duplicate on fresh plates for incubation at 30 and 42 °C to assay for complementation of growth at the nonpermissive temperature.

Automated Edman Degradation—For N-terminal protein sequence analysis, enzyme reaction mixtures were separated by SDS-PAGE and then transferred electrophoretically to polyvinylidene difluoride membranes. Transferred proteins were visualized on the polyvinylidene difluoride blots by staining with Coomassie Blue then excised for sequence analysis. N-terminal Edman degradations were performed using an Applied Biosystems Model 492 automated protein sequencer.

Matrix-assisted Laser Desorption Ionization Time-of-Flight (MALDI-TOF) Mass Spectrometry—SPase cleavage of proOmpA nuclease A was also analyzed using mass spectrometry. Small aliquots of reaction mixtures (10–20 μ l) were precipitated by the addition of 10 volumes of ice-cold acetone. After standing on ice for 10 min, the acetone-precipitated proteins were sedimented by centrifugation in an Eppendorf centrifuge at 13,000 rpm for 10 min. The supernatant was carefully removed by aspiration, and the protein pellets (usually not visible) were redissolved by the addition of 5 μ l of 10% formic acid. The dissolved proteins were mixed with the matrix solution: 5 μ l of saturated solution of α -cyano-4-hydroxycinnamic acid (10 mg dissolved in 500 μ l of 0.1% trifluoroacetic acid and 500 μ l of CH₃CN). The stainless steel MALDI-TOF target plate was spotted with 1 μ l of each reaction sample and analyzed using a Bruker Daltonics Autoflex mass spectrometer in the



Downloaded from www.jbc.org at University of British Columbia on June 11, 2008

Fig. 2. Effect of mutations that are predicted to increase or decrease the size of the binding pocket on SPase activity. *A*, mutations that are predicted to increase the size of the binding pocket. *P* indicates the position of the uncleaved preprotein, and *M* indicates the position of the mature protein. *B*, mutations that are predicted to decrease the size of the binding pocket. Wild-type PONA was digested by serial dilutions of stock wild-type and mutant forms of signal peptidase to study the effect of changing the size of the substrate binding pockets. The 0 dilution lane in the *upper gel* is a control in which no enzyme has been added and indicates the position of the unprocessed form of PONA. Processing of PONA was initiated by the addition of 1 μ l of signal peptidase stock (0.1 mg/ml) or a corresponding serial dilution of the stock to 10 μ l of PONA reaction mixture (0.04 mg/ml in 50 mM Tris, 10 mM CaCl₂, 1% Triton X-100, pH 8.0). Reactions were incubated for 1 h at 37 °C and then run on 17% SDS-PAGE.

linear mode. The instrument was calibrated with a mixture of protein standards including insulin (5,734.6 Da); cytochrome *c* (12,361.1 Da), and myoglobin (16,952.6 Da). The mass accuracy in the 17 kDa mass range was \pm 11 Da.

Prediction of Theoretical Mass for Cleavage Products—To predict the size of postulated cleavage products to match with the mass spectrometry data (see Table III), various portions of the sequence of the mature domain of proOmpA-Nuclease A were entered into the PeptideMass tool on the ExPASy Proteomics Server (us.expasy.org/tools/peptidemass.html). Singly charged average masses were calculated without enzymatic cutting to obtain the total mass of the predicted protein products of cleavage by signal peptidase.

Molecular Modeling—Models of each of the SPase mutants were made using the atomic coordinates from the recent crystal structure of signal peptidase in complex with a lipopeptide inhibitor (Protein Data Bank code 1T7D) as the template (19). The mutations were made with the program XtalView (20). The model for the proOmpA nuclease A (PONA) substrate was built into the active site of SPase using the acyl-enzyme penem inhibitor (10) and noncovalently bound lipopeptide inhibitor complexes (19) as a guide to position the P1 and P3 residues into the S1 and S3 binding pockets. The paths taken by the signal peptide along the surface of SPase and the parallel β -sheet type hydrogen bonding interactions with SPase are basically the same as those observed in the lipopeptide inhibitor complex structure. The models of

TABLE I
Activity of mutant SPases relative to WT SPase

Activities of mutant SPases were determined from dilution studies shown in Figure 2. Dilution of WT and mutant necessary to achieve 50% processing was determined and comparison yielded the relative activities.

| Mutant enzyme | Proposed pocket | Activity relative to 100% WT |
|---------------|-----------------|------------------------------|
| F84A | S3 | 50 |
| F84W | S3 | 10 |
| I86A | S1/S3 | 0.5 |
| G89A | S1 | 100 |
| M91A | S1 | 5 |
| L95A | S1 | 10 |
| L95R | S1 | 0 |
| I130A | S1 | 100 |
| V132A | S3 | 1 |
| V132I | S3 | 100 |
| D142E | S3 | 10 |
| D142I | S3 | 100 |
| Y143A | S1/S3 | 10 |
| Y143W | S1/S3 | 100 |
| I144A | S1/S3 | 50 |
| I144C | S1/S3 | 50 |
| I144S | S1/S3 | 10 |
| I144A/I86A | S1/S3 | 0.1 |

the SPase-PONA complexes were energy-minimized using the program CNS (21). Figures were prepared using the program PyMol (22).

RESULTS

In Vitro Analysis of SPase Binding Site Mutants with the Wild-type Preprotein Substrate—To test the importance of amino acids that comprise the S1 and S3 pockets for SPase catalysis, site-directed mutagenesis was used to alter substrate binding residues predicted to increase or decrease the size of the S1 and S3 pockets. The pocket residues were changed to alanines to increase the pocket size (Fig. 2A). Each of the mutant SPases was purified to homogeneity and then assayed using PONA with different dilutions of the SPase. The dilution factor required to achieve 50% processing can be used to estimate the relative activity of the mutant enzyme relative to the wild-type (WT) (Table I). The mutant with the lowest enzymatic activity was the I86A variant with a 200-fold lower activity relative to the wild-type enzyme. The L95A and M91A mutants were impaired roughly 10–20-fold when compared with the wild-type enzyme, whereas the V132A mutant exhibited a 100-fold decrease in activity. In contrast, the other mutants had near WT activity. To decrease the size of the S1 and S3 pockets, residues were changed to those indicated in Fig. 2B. As can be seen, these mutations that resulted in a smaller predicted pocket size had only a modest effect on the activity. Of these mutants, the F84W SPase was the most affected with an activity $\frac{1}{10}$ of that of the WT enzyme. The L95R SPase, which has an arginine introduced into the S1 substrate binding pocket, served as a negative control. Placement of Arg in this location was expected to interfere with the binding and structure of the enzyme. The L95R SPase had no measurable activity *in vitro*.

In Vitro Analysis of SPase Cleavage of Preprotein Substrate Mutants—As a first step to examine the substrate specificity of the different SPase mutants, we examined the ability of the WT and selected SPase mutants to process PONA substrates with different –1 or –3 residues (Fig. 3A). The WT SPase cleaved the WT PONA (with a –1 and –3 alanine) to generate the mature nuclease A domain. In contrast, the WT enzyme cleaved PONA with phenylalanine at the signal peptide –1 position to produce a product running slower on SDS-PAGE than the mature nuclease A domain. Alternatively, a PONA substrate with a –3 phenylalanine is cleaved by the WT SPase to produce a cleavage product of a similar size as that observed

with the WT substrate. A similar cleavage pattern is observed for the –3 Phe mutant with the other SPase mutants assayed. In contrast, the SPase I144A, I144C, and I144S mutants can cleave the –1 Val PONA to a rapidly migrating OmpA nuclease A like that observed when the WT SPase processes WT PONA. Only a small amount of cleavage of the –1 Val PONA mutant is observed with the double mutant I144A/I86A. With the –3 phenylalanine proOmpA nuclease A variant, all the I144 mutants produce a processed band similar in size to the wild-type. However, almost no processing of the –1 phenylalanine mutant is observed for any of these mutants.

We followed the time course of –1 Phe PONA processing using higher enzyme concentrations since very little processing of the PONA was observed for the Ile-144 mutants in lower enzyme concentrations. Indeed, cleavage is observed at these higher SPase levels for all of the mutants (Fig. 3B). Interestingly, a lower molecular weight processed band is observed when cleavage is performed with the WT, I144A, and I144S SPase enzymes. These studies showed that the WT and SPase mutants cleaved the PONA mutant substrates, but it was not clear where cleavage was occurring.

Mass Spectrometric Analysis of Signal Peptide Cleavage—To identify the sites of cleavage of the various substrates by the SPase enzymes, mass spectrometry was utilized to measure the masses of the major (Table II, major peak (*)) and minor products. The mass data are shown in Table II, and Table III shows the predicted theoretical masses corresponding to cleavage of the PONA substrates at various positions from –11 to +6. By comparing the mass data (Table II) with the theoretical masses (Table III) for processing at various sites, we determined where processing had occurred. For selected samples, Edman degradation was performed on the cleavage products to confirm the processing site. Edman degradation showed that the WT enzyme cleaved the WT PONA substrate exclusively at the predicted site. In addition, mass spectrometry showed that a peak at $16,812 \pm 11$ Da (16,812 Da theoretical) was produced by SPase cleavage (Fig. 4A), indicating cleavage at the predicted site. In contrast, WT SPase processed the –1 Phe mutant eight residues toward the N terminus from the wild type cleavage site following the Ala-Leu-Ala sequence. Edman degradation yielded the sequence, GFATVAQ. MALDI-TOF analysis determined a mass of 17,637 Da (17,634 Da theoretical) (Fig. 4B). Processing of the –1 Val substrate by WT SPase shows the majority of cleavage occurring at the same Ala-Leu-Ala sequence, in this case producing a peak of mass 17,601 Da (17,586 Da theoretical). For this digest, other minor cleavage products are observed as well with masses: 17,052, 17,810 and 16,651 corresponding to cleavage following –3 Ala (17,040 Da theoretical), –11 Ala (17,770 Da theoretical), and +2 Thr (16,640 Da theoretical).

In contrast to the fidelity seen when the WT SPase cleaves the wild-type PONA, the I144C mutant cleaved the same substrate at a number of sites, as determined by mass spectrometry. Although the major peak is at the normal cleavage site, significant cleavage was also observed at other sites (Fig. 4A). Mass analysis revealed a major product of 16,819 Da as well as alternate cleavage products of mass 17,028, 16,751, 16,646, and 16,559 Da (compare this with the WT, where only a 16,812 Da cleavage product is observed). Analysis of these data with the theoretical masses of various PONA cleavage products (Table III) revealed that cleavage occurred after the –3 Ala (17,011 Da theoretical), +1 Ala (16,741 Da), +2 Thr (16,640 Da), and +3 Ser (16,553 Da). A second trial digestion confirmed the results from the first trial, producing the same cleavage products (Table II). Multiple cleavage sites occurred as well with the –1 Phe PONA substrate by the I144C mutant (Table II). The first trial shows the following

FIG. 3. Processing of PONA with alternate -1 and -3 residues. WT and three PONA mutants, -1 Val, -1 Phe, and -3 Phe, were assayed for processing by the indicated SPase mutants. *A*, to demonstrate processing of PONA mutants, an overnight incubation was conducted. 0.5 μ g of SPase (WT or mutant) was added to the PONA reaction mixture (0.04 mg/ml in 50 mM Tris, 10 mM CaCl₂, 1% Triton X-100, pH 8.0) and incubated at 37 °C for 18 h. Samples were run on 17% SDS-PAGE and detected with silver staining. *P* indicates the position of the uncleaved preprotein, and *M* indicates the position of the cleaved protein band. *B*, to demonstrate the development of processed bands over extended incubations, reactions were set up as in Fig. 2 and incubated at 37 °C. At the designated time point, a portion was removed, and the reaction was stopped by the addition of denaturing loading buffer. All time points were then analyzed by 17% SDS-PAGE followed by silver staining.

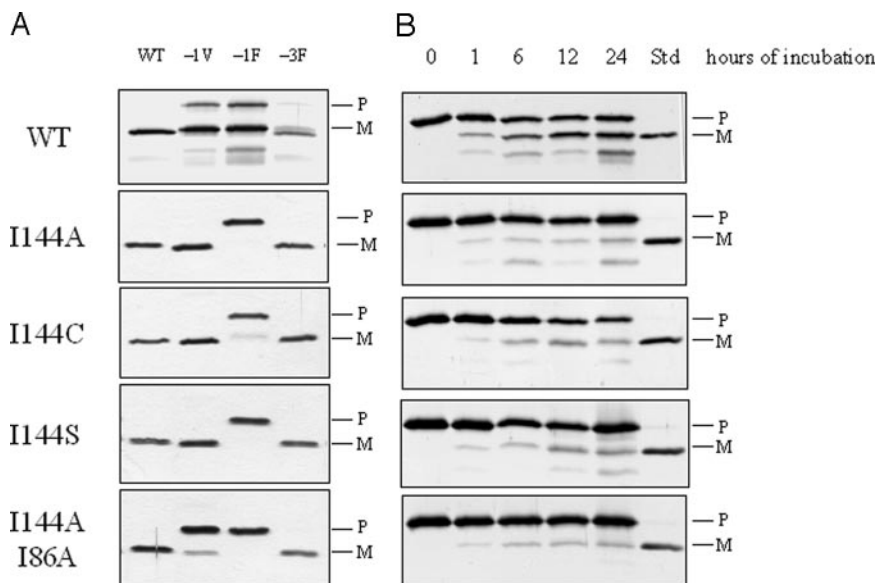


TABLE II
Mass spectral data of PONA cleavage products

Mass data for the major and minor peaks determined by mass spectrometry is tabulated below. The first entry in the column indicates the major peak (*) followed by any other minor peaks observed. Predicted masses for theoretical cleavage are indicated in parentheses.

| WT PONA | |
|---------------|--|
| WT SP | |
| 1 | *16812 (16812) |
| 2 | *16815 (16812) |
| I144C SP | |
| 1 | *16819 (16812), 16646 (16640), 16751 (16741), 16559 (16553), 17028 (17012) |
| 2 | *16823 (16812), 16651 (16640), 16754 (16741), 16565 (16553), 17031 (17012) |
| I144A/I86A SP | *16812 (16812) |
| I144C/I86C SP | *16819 (16812) |
| I144C/I86T SP | *16822 (16812), 17033 (17012) |
| -1F PONA | |
| WT SP | |
| 1 | *17637 (17634), 17081 (17088) |
| 2 | *17639 (17634), 17085 (17088) |
| I144C SP | |
| 1 | *17075 (17088), 16808 (16812), 16547 (16553), 17628 (17634) |
| 2 | *16550 (16553), 16637 (16640), 16738 (16741) |
| I144A/I86A SP | *16808 (16812) |
| 1 | *16817 (16812) |
| -1V PONA | |
| WT SP | *17601 (17586), 17052 (17040), 17810 (17770), 16651 (16640) |
| I144A SP | *16648 (16640), 16852 (16812) |
| I144C SP | *16645 (16640), 16818 (16812) |
| I144S SP | *16651 (16640), 16837 (16812) |
| I144A/I86A SP | *16646 (16640) |
| -1N PONA | |
| WT SP | *17067 (17055), 16825 (16812) |
| I144A SP | *16828 (16812), 17049 (17055) |
| I144C SP | *16823 (16812) |
| I144S SP | *16826 (16812) |
| I144A/I86A SP | *16825 (16812) |
| I144C/I86C SP | *16825 (16812), 17067 (17055) |
| I144C/I86T SP | *16827 (16812), 17045 (17055) |
| -3F PONA | |
| WT SP | *16652 (16640), 17643 (17634) |
| I144A SP | *16647 (16640) |
| I144C SP | *16653 (16640) |
| I144S SP | *16645 (16640) |
| I144A/I86A SP | *16658 (16640), 16864 (16883) |

peaks: 17,075, 16,808, 16,547, and 17,628 Da. Analysis of these masses showed corresponding cleavage sites after -3 Ala (17,088 Da theoretical), -1 Phe (16,812 Da), +3 Ser (16,553 Da), as well as the upstream -9 Ala (17,634 Da) site seen with the WT enzyme. The second trial showed a different pattern: 16,550, 16,637, and 16,738 Da with major cleavage occurring after +3

Ser (16,553 Da theoretical), +2 Thr (16,640 Da), and +1 Ala (16,741 Da). Taken together, the results demonstrate that the Ile-144 residue is important for determining the accuracy of SPase cleavage.

Although the I144C mutant loses its fidelity of cleavage, the I144A/I86A mutant cleaved the WT PONA substrate only at

TABLE III
Predicted theoretical masses of various PONA cleavage products

The theoretical masses of possible PONA cleavage products were predicted using the PeptideMass tool on the ExPASy Proteomics Server. Average masses are reported as $[M + H]^+$.

| AA Sequence | Name | WT | -1V | -1F | -1N | -3F |
|--------------------------|------|----------|----------|----------|----------|----------|
| M (H)6 K K T A I A I A V | | 19,663.6 | 19,691.7 | 19,739.7 | 19,706.6 | 19,739.7 |
| A | -11 | 17,813.4 | 17,841.5 | 17,889.5 | 17,856.4 | 17,889.5 |
| L | -10 | 17,742.4 | 17,770.4 | 17,818.4 | 17,785.4 | 17,818.5 |
| A | -9 | 17,629.2 | 17,657.2 | 17,705.3 | 17,672.2 | 17,705.3 |
| G | -8 | 17,558.1 | 17,586.2 | 17,634.2 | 17,601.1 | 17,634.2 |
| F | -7 | 17,501.1 | 17,529.1 | 17,577.2 | 17,544.1 | 17,577.2 |
| A | -6 | 17,353.9 | 17,381.9 | 17,430.0 | 17,396.9 | 17,430.0 |
| T | -5 | 17,282.8 | 17,310.9 | 17,358.9 | 17,325.8 | 17,358.9 |
| V | -4 | 17,181.7 | 17,209.8 | 17,257.8 | 17,224.7 | 17,257.8 |
| A (F) | -3 | 17,082.6 | 17,110.6 | 17,158.7 | 17,125.6 | 17,158.7 |
| Q | -2 | 17,011.5 | 17,039.5 | 17,087.6 | 17,054.5 | 17,011.5 |
| A (V, F, or N) | -1 | 16,883.4 | 16,911.4 | 16,959.5 | 16,926.4 | 16,883.4 |
| A | +1 | 16,812.3 | 16,812.3 | 16,812.3 | 16,812.3 | 16,812.3 |
| T | +2 | 16,741.2 | 16,741.2 | 16,741.2 | 16,741.2 | 16,741.2 |
| S | +3 | 16,640.1 | 16,640.1 | 16,640.1 | 16,640.1 | 16,640.1 |
| T | +4 | 16,553.0 | 16,553.0 | 16,553.0 | 16,553.0 | 16,553.0 |
| K | +5 | 16,451.9 | 16,451.9 | 16,451.9 | 16,451.9 | 16,451.9 |
| K | +6 | 16,323.7 | 16,323.7 | 16,323.7 | 16,323.7 | 16,323.7 |
| -PONA | | 16,195.6 | 16,195.6 | 16,195.6 | 16,195.6 | 16,195.6 |

the correct site producing a mass of 16,812 Da (theoretical 16,812 Da) (Table II). Strikingly, this double mutant also cleaves the -1 Phe PONA at the correct cleavage site position (following the -1 Phe), generating a 16,808 Da product in our first trial and a 16,817 Da product in the second trial, both closely matching the predicted mass of 16,812 Da within the error range of ± 11 Da. Due to the fact that the -1 Phe PONA is a poor substrate, some of the uncleaved preprotein of theoretical mass 19,740 Da is observed in both spectra (Fig. 4B). This demonstrates that the specificity of the SPase mutant has been changed.

A different cleavage pattern was observed for the Ile-144 mutants processing the -1 Val PONA. None of the mutants were capable of efficient cleavage following the -1 Val, with only I144A, I144C, and I144S showing cleavage at this site to a very limited extent. Cleavage occurred almost exclusively after the +2 Thr, according to mass spectrometry. Edman degradation was performed, and the results showed that the substrate was cleaved by I144C after the sequence Val-Ala-Thr (after the +2 site); a very weak sequence was observed: Ser-Thr-X-X-Leu-X-X-Glu-Ala.

Similar results were observed for the processing of the -3 Phe substrate. Mass analysis confirmed cleavage after the +2 Thr residue for the WT SPase in addition to the I144A, I144C, I144S, and I144A/I86A mutants (Table II). Limited processing is also observed at the -9 Ala (17,643 Da) site when WT SPase is incubated with this substrate.

Fig. 5 shows processing of different substrates using serial dilutions of the WT and mutant SPases to determine the efficiency of cleavage of SPase and substrate pairs. As can be seen, the I144A, I144C, and I144S SPase mutants have roughly $\frac{1}{10}$ of the activity when compared with the WT SPase in cleaving the WT substrate (Fig. 5A). In contrast, the I144A/I86A mutant has roughly $\frac{1}{1000}$ the activity for cleaving the WT substrate relative to the WT SPase. Even greater reduction in activity is seen toward the mutant substrates (Fig. 5B). Processing is highly impaired for the WT and mutant SPases in cleaving the -1 Phe substrate. Only a small amount of processing is observed at the highest enzyme level. This indicates that for the WT enzyme, the WT substrate is preferred more than 10,000-fold over the -1 Phe substrate. Also, when cleavage occurs, it is at the alternative upstream site. Likewise, the single Ile-144 mutants have roughly 1000-fold preference for cleaving the WT PONA over the -1 Phe PONA. Although not as pronounced for

the other tested SPases, there is a preference for cleavage of the WT substrate over the -1 Phe substrate even for the I144A/I86A SPase. Similarly, cleavage of PONA with a -1 Val or -3 Phe is strongly reduced relative to the wild type.

Since the I144A/I86A mutant has a change of specificity, it is evident that the Ile-144 and Ile-86 residues are important for substrate specificity in SPase. It is remarkable that Imp1, which is the only member of the SPase family to possess unusual substrate specificity, cleaving after a -1 asparagine, has different residues at the homologous 144 and 86 positions than other members of the family. Instead of an isoleucine at the homologous 144 position, it has a cysteine. At the homologous 86 position, it has either a cysteine or a threonine, not an isoleucine. Therefore, we constructed SPase mutants incorporating cysteine or threonine at the homologous positions to generate the two double mutants: I144C/I86C and I144C/I86T. These mutants along with WT SPase were assayed for their ability to cleave the WT and -1 Asn PONA in a dilution study as described above (Fig. 6). In processing the WT PONA, both mutants are clearly impaired, exhibiting a 1000-fold reduction with the I144C/I86T mutant being slightly more active (Fig. 6A). When the activities are compared for the processing of -1 Asn PONA, all three enzymes exhibit very low activity, showing processing at only the most concentrated enzyme condition. However, the activities are now quite similar for the WT and these two mutants. In switching substrates from WT to -1 Asn, the WT SPase activity has been reduced 10,000-fold, whereas the I144C/I86C and I144C/I86T mutants have suffered only around an order of magnitude loss in activity.

Processing of the -1 Asn PONA by the WT and mutant SPase was observed at two discrete sites (Table II). The digest of -1 Asn PONA with WT enzyme yielded a mixture of products; the major peak was 17,067 Da, which corresponds to processing upstream after the -3 Ala (17,055 Da theoretical). Surprisingly, the minor peak occurred at 16,825 Da, which is in close agreement to the theoretical mass of 16,812 Da for processing following the -1 Asn residue. This is an unanticipated result as processing following -1 Asn has not been observed previously for WT SPase (12, 13). In the I144C/I86C and I144C/I86T digests, these same peaks were observed. However, in the case of these mutants, the major peak is the one representing cleavage following -1 Asn (Fig. 4C). In addition, cleavage following the -1 Asn as the major product was observed with all the Ile-144 mutants and the I144A/I86A mutant (Table II).

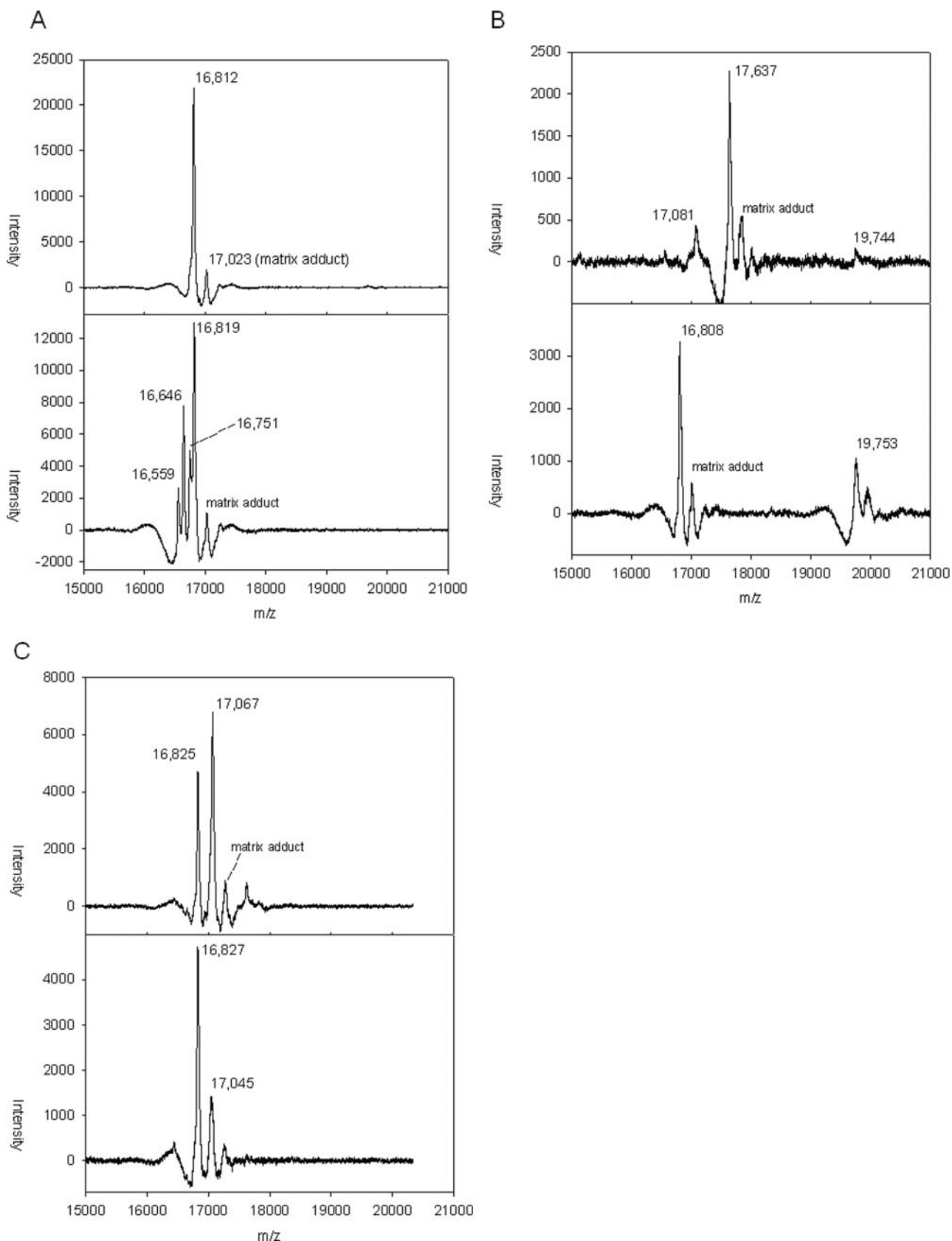


FIG. 4. Mass analysis demonstrates altered cleavage profile for SPase mutants. Selected mass spectra are paired to illustrate alteration in PONA processing in the various SPase mutants. *A*, processing of WT PONA by WT SPase yields a single peak corresponding to the WT cleavage product (17,023 is the peak due to the matrix adduct). In the *lower panel*, digestion by I144C SPase shows multiple peaks, demonstrating a loss of fidelity. *B*, in the *upper panel*, processing of the -1 Phe PONA by the WT enzyme yields peaks, which are heavier than the product corresponding to cleavage at the -1 site, indicating selection of alternate processing sites. In contrast, the I144A/I86A mutant shows cleavage following the -1F residue (*lower panel*). *C*, mass spectra data from digestion of -1 Asn PONA by the WT and I144C/I86T SPase are shown. Processing is observed following the -1 Asn and -3 Ala residues in both cases. In the *lower panel*, the shift in relative intensity of the peaks indicates a change in preference for the -1 Asn cleavage site for the I144C/I86T mutant.

FIG. 5. Activity of SPase (SP) mutants with the WT and mutant PONA substrates. The dilution series experiment was repeated as described in the legend for Fig. 2 utilizing the -1 Val, -1 Phe, and -3 Phe PONA mutants in addition to WT. *A*, for the processing of WT PONA, all dilution lanes are shown, whereas in *B*, only the 1 (or undiluted) lane is shown for the mutants due to their low observed activity. *P* indicates the position of the uncleaved preprotein, and *M* indicates the position of the mature protein.

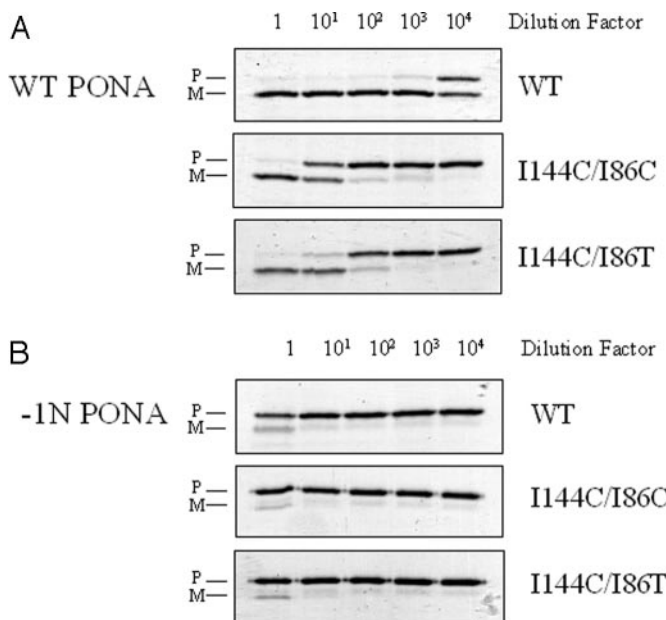
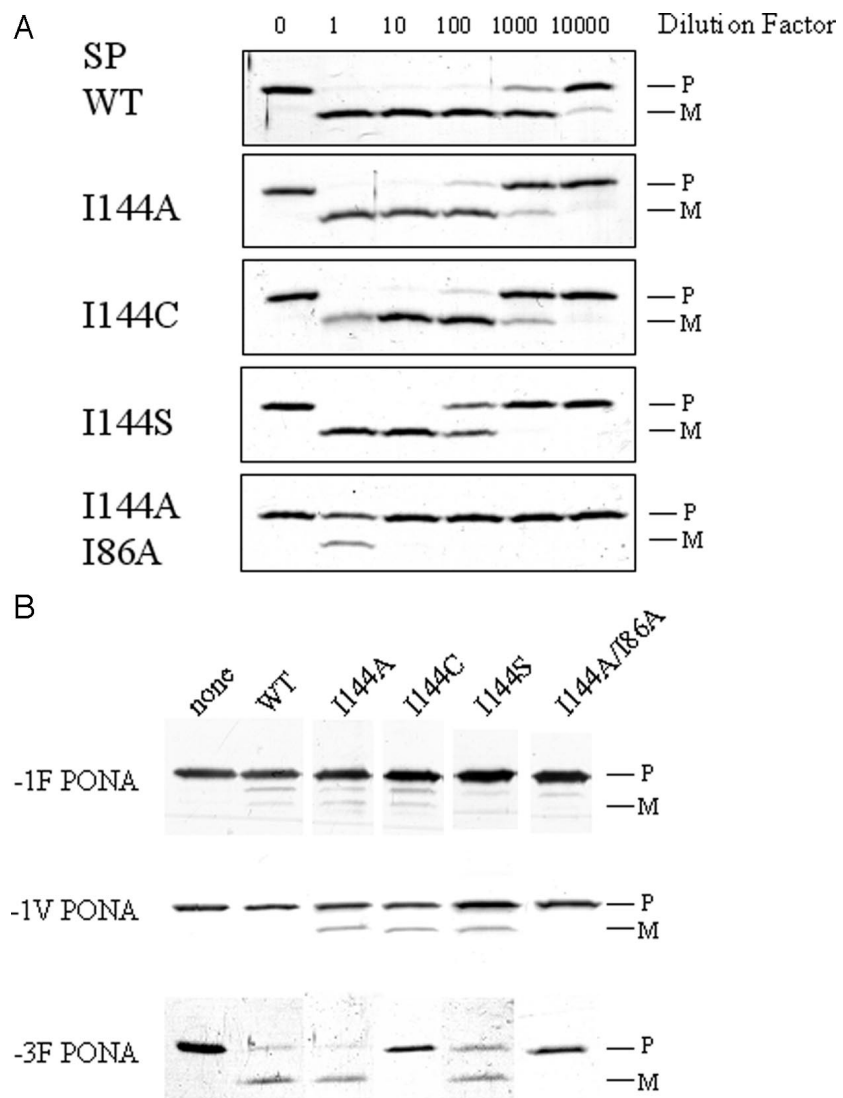


FIG. 6. Processing of WT and -1 Asn PONA substrates by WT, I144C/I86C, and I144C/I86T mutants. The dilution series experiment was conducted as in Fig. 2 using the WT (*A*) and -1 Asn (*B*) PONA substrates. *P* indicates the position of the uncleaved preprotein, and *M* indicates the position of the mature protein.

In Vivo Analysis of Signal Peptidase Binding Site Mutants—To investigate how detrimental the SPase mutations would be with the proteins in the natural membrane environment, we examined processing of proOmpA *in vivo* using the temperature-sensitive IT41 strain (15), modified by the incorporation of the T7 RNA polymerase as described above. IT41(DE3) was grown in M9+glucose medium at 30°C to a density of $0.3 A_{600}$ and then shifted to 42°C for 1.5 h. The cells were pulsed with [^{35}S]methionine for 10 s and then chased with nonradioactive methionine for the indicated times. Fig. 7 shows that the processing of proOmpA is dramatically delayed. However, IT41(DE3) bearing a plasmid encoding WT SPase shows rapid processing. I86A SPase, which showed $\frac{1}{1000}$ the activity as WT enzyme in a detergent extract with proOmpA nuclease A, was active *in vivo*. Processing was completely normal at the nonpermissive temperature when IT41(DE3) was transformed with a plasmid expressing I86A SPase. No *in vivo* activity was observed for L95R and active site residue mutant, K145A. Except for the L95R SPase mutant, all of the SPase mutants with substrate binding pocket mutations showed activity *in vivo* (Table IV).

Complementation of the growth defect of IT41(DE3) at 42°C was assayed for all the SPase mutants. Most mutants clearly showed complementation in this experiment with equivalent colonies on both 30 and 42°C plates. Other mutants showed a reduced number of colonies on the 42°C plate, whereas still

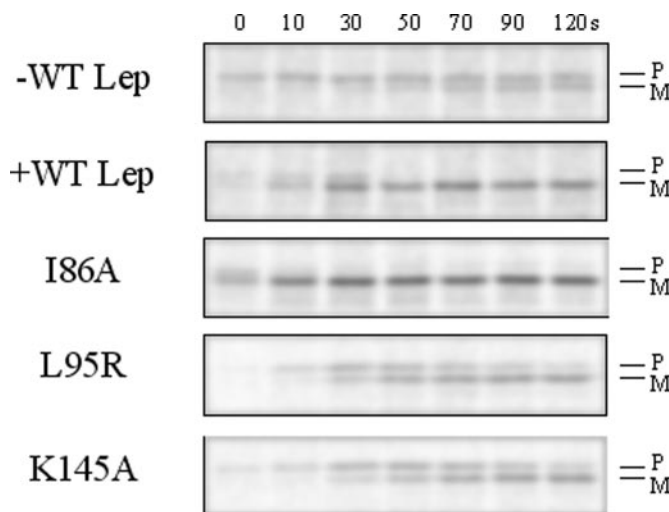


FIG. 7. In vivo complementation of OmpA processing defect in IT41(DE3) at 42 °C. SPase mutants were studied for their ability to complement for the temperature-sensitive SPase defect of IT41(DE3) at 42 °C. Only fresh transformants of SPase and SPase mutants into IT41(DE3) were used. Colonies incubated at 30 °C (see “Experimental Procedures”) were transferred to 2 ml of M9 +glucose medium and incubated at 30 °C until a density of 0.3 A_{600} was reached. The cultures were then shifted to a 42 °C incubator and incubated for an additional 1.5 h. Cell cultures were labeled with [35 S]methionine for 10 s, at which time the 0 time point was taken. After the 0 time point was taken, the chase was begun with the addition of excess nonradioactive methionine with additional time points taken at indicated times. At each time point, 250 μ l of culture was quenched by addition to 250 μ l of ice-cold 20% trichloroacetic acid. These were then subjected to immunoprecipitation with OmpA antiserum (see “Experimental Procedures”) and run on 15% SDS-PAGE. *P* indicates the position of the uncleaved proOmpA protein, and *M* indicates the position of mature OmpA.

TABLE IV

In vivo processing of *proOmpA* in the temperature sensitive strain IT41(DE3) at the nonpermissive temperature 42 °C

The following mutants exhibited 50% processing in <10 s like WT SP: F84A, F84W, G89A, I86A, M91A, M91I, L95A, V103I, I130A, V132A, V132I, D142E, D142I, Y143A and I144A. This table indicates the amount of chase time required to observe 50% processing for the WT and mutant SPases. Times are indicated in seconds of chase.

| Lep Mutant | Time point of 50% processing |
|--------------------|------------------------------|
| | s |
| No plasmid control | 120 |
| WT (+control) | <10 |
| I144A/I86A | 10 |
| L95R | 50 |
| K145A (-control) | 70 |

others exhibited poorly reproducible growth. Throughout this study, the binding pocket mutant, L95R, and active site mutant, K145A, negative controls exhibited no growth at 42 °C in any of the trials conducted. These results indicate that the mutants, although impaired to varying degrees in their *in vitro* activities, can still complement *in vivo* in most cases, whereas the negative controls clearly cannot.

Molecular Modeling of Binding Site Mutants of Signal Peptidase Binding in Complex with Signal Peptides—To help in the interpretation of the mutations made both within the binding pockets of SPase and within the recognition residues of the PONA substrate, we have modeled the SPase-PONA complex. The models use the recently solved crystal structure of the complex between signal peptidase and the lipopeptide Arylomycin A₂ as the template (Protein Data Bank code 1T7D) (19). As described under “Experimental Procedures,” the model for PONA was built into the active site of SPase using the acyl-enzyme penem inhibitor crystal structure and noncovalently

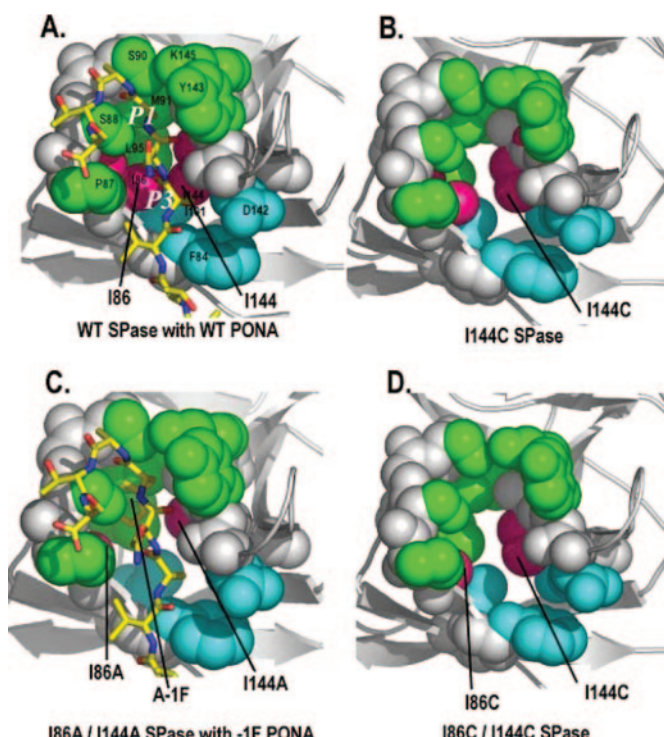


FIG. 8. Molecular modeling of binding site mutants within *E. coli* signal peptidase. The amino acid residues of signal peptidase that contribute to the binding pocket surface are shown in van der Waals spheres. The side chain atoms from those residues that contribute to the S1 binding pocket (Pro-87, Ser-88, Gly-89, Ser-90, Met-91, Leu-95, Tyr-143, Lys-145) are colored green. The side chain atoms from those residues that contribute to the S3 binding pocket (Phe-84, Ile-101, Val-132, Asp-142) are colored cyan. The side chain atoms from those residues that contribute to both the S1 and the S3 binding pockets (Ile-86 and Ile-144) are colored hot pink. The main chain atoms are colored white. The P3' to P5' residues of the PONA substrate are shown in yellow (carbon), blue (nitrogen), and red (oxygen). *A*, the wild-type signal peptidase with wild-type proOmpA nuclease A. *B*, the I144C mutant of signal peptidase. *C*, the I86A/I144A mutant of signal peptidase with the bound P1 Ala to P1 Phe mutant of proOmpA nuclease A. *D*, the I86C, I144C mutant of signal peptidase.

bound lipopeptide inhibitor complex crystal structure as a guide to position the P1 and P3 residues into the S1 and S3 binding pockets. The path taken by the substrate along the surface of SPase and the nonspecific binding interactions with SPase are basically the same as those observed in the lipopeptide inhibitor complex structure. The ribbon diagram of WT SPase in complex with the WT PONA signal peptide is shown (Fig. 1). PONA makes parallel β -sheet interactions with the strands that line the binding sites (residues 83–90 and 142–145) (Fig. 1*B*). As can be seen from Figs. 1*B* and 8*A*, the P1 Ala residue points into the S1 pocket, and the P3 Ala points into the shallow S3 pocket. The residues Ile-86 and Ile-144 sit just at the borderline between the S1 and S3 pockets and contribute atoms to both pockets. The change in the volume of the binding pockets can be seen when the residues contributing to the binding site are depicted in van der Waals spheres (Fig. 8). The ability of the double mutant I86A/I144A to cleave a PONA substrate with a -1 Phe can be rationalized from the modeling, which shows the increased volume within the S1 binding pocket provided by the isoleucine to alanine substitutions, allows the phenyl side chain to fit into the pocket without any van der Waals clashes (Fig. 8*C*). A similar reasoning based on steric effects can be used to explain the ability of the I86C/I144C to bind and cleave PONA substrates with a -1 Asn (Fig. 8*D*). It is not clear from the molecular modeling why the mutant I144C (Fig. 8*B*) has the ability to cleave at multiple sites

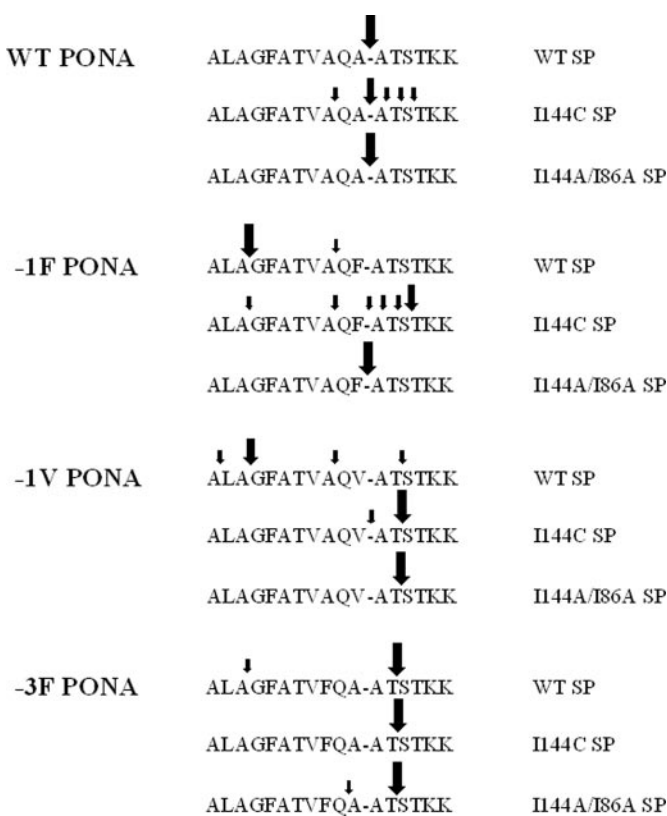


FIG. 9. The cleavage site of signal peptide mutants by various signal peptidase mutants. The peptide sequence of the WT PONA and each PONA mutant construct is listed in addition to the processing sites observed for each indicated SPase enzyme. Arrows indicate the site of processing, and the relative sizes of the arrows indicate major and minor peaks.

within PONA substrate.

DISCUSSION

Here we investigated which residues within the substrate binding pocket of SPase are responsible for the high fidelity of SPase and contribute to the substrate specificity of SPase. Toward this objective, we changed all the candidate S1 and S3 residues within SPase that are believed to bind to the -1 and -3 residues of the precursor substrate. Changes were made that were designed to either increase or decrease the size of the binding pocket. With the exception of the I86A SPase mutant, the results of increasing the size of the pocket showed that most of the mutants were still quite capable of cleaving the substrate, with only a few mutants demonstrating a 10–20-fold reduction in activity. These results suggest that there is plasticity in the substrate binding pocket. The mutants that were designed to decrease the size of the substrate binding pocket again only had modest effects. This is probably due to the fact that the pockets are already quite small within the WT SPase and that the enzyme is most likely able to make the necessary structural adjustments required to bind the mutant substrates. A comparison of the three crystal structures so far available for the *E. coli* signal peptidase (the apo-enzyme (23), the covalently bound acyl-enzyme inhibitor complex (10), and the noncovalently bound peptide inhibitor form (19)) show that adjustments in both the main chains and side chains surrounding the binding site are observed (19).

Our results showed that mutation of isoleucine 144 to cysteine alters the fidelity of the enzyme. The I144C SP cleaved not only at the normal processing site but also at other sites: after the -3 Ala, -1 Ala, $+1$ Ala, $+2$ Thr, and $+3$ Ser with respect to the normal cleavage position (Fig. 9 shows a cleavage

site summary). The proximal sequences including the cleavage sites are: TVA-Q for the -3 Ala; AQA-A for the -1 Ala; QAA-T for the $+1$ Ala; AAT-S for the $+2$ Thr; and ATS-T for $+3$ Ser, where the $-$ indicates the position of cleavage. One possible explanation for this lack of fidelity may be that the cysteine mutation in the binding pocket may lead to sliding of the prebound substrate within the active site region. Sliding of the substrate once prebound would lead to a cleavage profile with sites clustered around the canonical site as observed in our experiments. The WT leucine in the substrate binding pocket leads to optimal binding, which prevents sliding, and thereby cleavage occurs at only the normal site. These results support the idea that the isoleucine 144 residue is important for SPase to cleave its substrate accurately at the proper site.

In addition to identifying a residue contributing to the accuracy of SPase cleavage, we identified residues that contribute to the substrate specificity of SPase. As mentioned in the introduction, the substrate specificity determinants of this enzyme are at the -1 and -3 position of the substrate protein. Signal sequences within preproteins contain a -1 Ala, Gly, Ser, and Thr and a -3 Ala, Val, Ser, Thr, Gly, and Leu (24). The *E. coli* SPase has been shown to cleave precursor substrates with a -1 Ala, Gly, Ser, Cys, Pro and, in some cases, Thr (12–14). In addition, it can cleave substrates with a -3 Gly, Leu, Val, Thr, Cys, Ser, Ile, Pro, and Asn. In bacteria, Phe is never found at the -1 or -3 position (25). Out of 334 Gram-negative signal peptide sequences in the Swiss-Prot data set, there are two Val and one Asn at the -1 position (25). However, they are believed to be incorrectly assigned signal peptidase cleavage site residues (25). Strikingly, the substrate specificity of SPase is changed with the mutation of the Ile-144 and Ile-86 residues to alanine. Although the WT enzyme cannot cleave the proOmpA nuclease substrate after the -1 Phe, the I86A/I144A mutant cleaved the substrate after the -1 Phe with no other cleavage products observed by mass spectrometry (Figs. 4B and 9). On the other hand, the WT SPase cleaved the -1 Phe substrate at an alternative site eight residues upstream (following the -9 Ala) from the normal cleavage site, following the standard processing rules. This suggests that residues well into the proposed signal peptide hydrophobic helical region of these mutant substrates are able to melt into the appropriate β -strand conformation needed to make the intermolecular contacts with the SPase binding site. Previously, processing at an alternative site has been observed when processing at the normal site was prevented by mutating the -1 residues (12). The I144C mutant cleaves the -1 Phe PONA substrate at multiple sites, again showing inaccuracy in cleavage of the substrates.

Although I144A/I86A SPase can cleave after -1 Phe, it is a very poor enzyme. Its activity is around $1/10,000$ when compared with the WT enzyme processing the WT proOmpA nuclease A substrate. A similar large reduction in activity was found with trypsin when the active site Gly-226 was changed to an Ala, resulting in increased preference for cleaving substrates with lysines relative to arginines (26). In addition, the substrate specificity of granzyme B can be extended at the P4 position (but the activity is lowered dramatically from 10- to 100-fold) by mutating the active site residues Ile-99 and Asn-218 to Ala residues (27). Further changes in the SPase protein, both in the active site and out of the active site region, may be necessary to increase the catalytic potency toward the -1 Phe substrate.

Our results indicate that the -1 and -3 residues within the PONA substrate strongly influence where the WT SPase cleaves the substrate. Although the WT SPase cleaves the -1 Val and -3 Phe substrates downstream within the mature domain at the cleavage sites, VAT-S and AAT-S, respectively

(Fig. 3A and Table II), it cleaves the -1 Phe PONA substrate eight residues upstream (from the normal cleavage site) within the leader sequence at ALA-G. For this substrate, WT SPase cannot cleave after the $+2$ Thr because the F is an inappropriate -3 residue (FAT-S), thereby preventing cleavage at this site (24).

A similarly strong influence of the $-1/-3$ residue is seen with the I144C and I144A/I86A SPases. The -1 Val PONA is processed by the SPase mutants mainly after the $+2$ Thr residue (following the cleavage sequence VAT-S), although I144C processing yielded at least one other minor peak, indicating cleavage after the -1 Val. Cleavage of the -1 Val PONA by the I144A/I86A mutant occurs at the VAT-S site exclusively over the normal cleavage position at -1 . This is in contrast to the AQF-A cleavage site observed with the -1 Phe PONA where SPase I144A/I86A cleavage does occur after the -1 position. It appears that in this case as well, the binding of valine by the S1 pocket is highly unfavorable, causing the shift to the VAT-S site. In addition, the -3 Phe PONA is processed by the WT, I144C, and I144A/I86A almost exclusively after the $+2$ Thr. Cleavage does not occur at the WT processing site because the -3 Phe is inappropriate for the signal peptidase specificity.

The cleavage of all the mutant substrates by WT and the tested SPase mutants is very poor (Fig. 5B), although cleavage is occurring at alternative sites (with the exception of -1 F mutant and I86A/I144A, which cleaves at the normal position after -1 Phe) following the SPase -1 , -3 processing rule of von Heijne and co-workers (24). This shows clearly that there is a positional dependence for the cleavage efficiency by SPase (normal position *versus* alternate position). However, it is perplexing that the I144C SPase mutant can cleave within the WT substrate at multiple sites quite efficiently. A possible explanation for this result is that the WT substrate first binds to SPase in a normal fashion via the -1 and -3 residue of the substrate and then slides in the active site area, allowing cleavage at the alternative sites. The cleavage products observed suggest that the active site of the enzyme preferentially slides into the mature domain to the next most preferred binding site, which in the case of I144C SPase results in cleavage following the $+2$ Thr. This is observed for the other PONA mutants as well, except in the case of the -1 F substrate, where cleavage following the $+2$ Thr places the engineered -1 F interacting unfavorably with the P3 SPase binding pocket. In this case, the enzyme preferentially cleaves following the next residue, $+3$ Ser.

The results with the I86A/I144A SPase and the -1 F PONA substrate show that the Ile-144 and Ile-86 residues of SPase play a central role in the process of accurately cleaving the preprotein substrate; change in the Ile-144 and Ile-86 residues effects a change in -1 , -3 substrate recognition. In light of this result, we observe an interesting correlation with the only SPase that exhibits a significantly altered substrate recognition sequence, Imp1 mitochondrial protease. Imp1 protease lacks the conserved 144 and 86 residues. Ile-144 is a cysteine residue, and Ile-86 is either a cysteine or a threonine residue. The result is an enzyme that cleaves *in vivo* after a -1 Asn cleavage site, which is unique among SPases (28, 29). The SPase mutants constructed to resemble the Imp 1 enzyme, I144C/I86C and I144C/I86T, yielded interesting results in the digestion of the -1 Asn PONA substrate. This analysis shows that both enzymes, in addition to WT SPase, produce the same two cleavage products. Processing was observed following the -3 Ala and -1 Asn residues. The proportions, however, are different with the WT enzyme selecting the -3 Ala site preferentially, whereas both Imp 1-type double mutants and other

Ile-144 mutants (data not shown) demonstrated a preference for cleavage following -1 Asn. WT SPase cleaves WT PONA 10,000 times better than the -1 Asn PONA. In contrast, the SPase Ile-144/Ile-86 mutants mimicking the Imp1 binding residues cleave WT PONA only 100 times better. Taken together, these observations strengthen the body of evidence that these residues, in particular, hold a special importance in determining the -1 , -3 substrate recognition sequence.

Future studies will have to examine the substrate specificity of the SPase with the Imp1 Ile-144/Ile-86 residues. Chen *et al.* (9) have shown that, in addition to cleaving its endogenous substrate, i-cyt b2, with a -1 Asn, Imp1 can process substrates with a -1 Ser, Cys, Met, Ala, and Leu. In addition, we will analyze the SPase S1 and S3 mutants, utilizing a library of peptide substrates with random sequence surrounding the OmpA cleavage site. These experiments hold the promise of identifying differences in the preferred cleavage sequence for each of the mutants, which is not possible using designed substrate sequences alone. These future data could help in clarifying the effects on substrate selection and fidelity observed in the current studies. In addition, crystallographic and spectroscopic analysis of these binding site mutants in complex with substrate mutants will help in the understanding of this interesting molecular recognition event that most likely occurs at or within the membrane surface.

REFERENCES

1. Paetzel, M., Karla, A., Strynadka, N. C., and Dalbey, R. E. (2002) *Chem. Rev.* **102**, 4549–4580
2. Tjalsma, H., Bolhuis, A., Jongbloed, J. D., Bron, S., and van Dijl, J. M. (2000) *Microbiol. Mol. Biol. Rev.* **64**, 515–547
3. Sung, M., and Dalbey, R. E. (1992) *J. Biol. Chem.* **267**, 13154–13159
4. VanValkenburgh, C., Chen, X., Mullins, C., Fang, H., and Green, N. (1999) *J. Biol. Chem.* **274**, 11519–11525
5. Black, M. T. (1993) *J. Bacteriol.* **175**, 4957–4961
6. Tschantz, W. R., Sung, M., Delgado-Partin, V. M., and Dalbey, R. E. (1993) *J. Biol. Chem.* **268**, 27349–27354
7. van Dijl, J. M., de Jong, A., Venema, G., and Bron, S. (1995) *J. Biol. Chem.* **270**, 3611–3618
8. Barbrook, A. C., Packer, J. C., and Howe, C. J. (1996) *FEBS Lett.* **398**, 198–200
9. Chen, X., Van Valkenburgh, C., Fang, H., and Green, N. (1999) *J. Biol. Chem.* **274**, 37750–37754
10. Paetzel, M., Dalbey, R. E., and Strynadka, N. C. (1998) *Nature* **396**, 186–190; Erratum (1998) *Nature* **396**, 707
11. Dierstein, R., and Wickner, W. (1986) *EMBO J.* **5**, 427–431
12. Fikes, J. D., Barkocy-Gallagher, G. A., Klapper, D. G., and Bassford, P. J., Jr. (1990) *J. Biol. Chem.* **265**, 3417–3423
13. Shen, L. M., Lee, J. I., Cheng, S. Y., Jutte, H., Kuhn, A., and Dalbey, R. E. (1991) *Biochemistry* **30**, 11775–11781
14. Karamyshev, A. L., Karamysheva, Z. N., Kajava, A. V., Ksenzenko, V. N., and Nesmeyanova, M. A. (1998) *J. Mol. Biol.* **277**, 859–870
15. Inada, T., Court, D. L., Ito, K., and Nakamura, Y. (1989) *J. Bacteriol.* **171**, 585–587
16. Klenotic, P. A., Carlos, J. L., Samuelson, J. C., Schuenemann, T. A., Tschantz, W. R., Paetzel, M., Strynadka, N. C., and Dalbey, R. E. (2000) *J. Biol. Chem.* **275**, 6490–6498
17. Takahara, M., Hibler, D. W., Barr, P. J., Gerlt, J. A., and Inouye, M. (1985) *J. Biol. Chem.* **260**, 2670–2674
18. Carlos, J. L., Paetzel, M., Brubaker, G., Karla, A., Ashwell, C. M., Lively, M. O., Cao, G., Bullinger, P., and Dalbey, R. E. (2000) *J. Biol. Chem.* **275**, 38813–38822
19. Paetzel, M., Goodall, J. J., Kania, M., Dalbey, R. E., and Page, M. G. (2004) *J. Biol. Chem.* **279**, 30781–30790
20. McRee, D. E. (1999) *J. Struct. Biol.* **125**, 156–165
21. Brunger, A. T., Adams, P. D., Clore, G. M., DeLano, W. L., Gros, P., Gross-Kunstleve, R. W., Jiang, J. S., Kuszewski, J., Nilges, M., Pannu, N. S., Read, R. J., Rice, L. M., Simonson, T., and Warren, G. L. (1998) *Acta Crystallogr. Sect. D Biol. Crystallogr.* **54**, 905–921
22. DeLano, W. L. (2002) PyMol, Ed. 0.96., DeLano Scientific, San Carlos, CA
23. Paetzel, M., Dalbey, R. E., and Strynadka, N. C. (2002) *J. Biol. Chem.* **277**, 9512–9519
24. Nielsen, H., Engelbrecht, J., Brunak, S., and von Heijne, G. (1997) *Protein Eng.* **10**, 1–6
25. Bendtsen, J. D., Nielsen, H., von Heijne, G., and Brunak, S. (2004) *J. Mol. Biol.* **340**, 783–795
26. Craik, C. S., Largman, C., Fletcher, T., Rocznak, S., Barr, P. J., Fletterick, R., and Rutter, W. J. (1985) *Science* **238**, 291–297
27. Ruggles, S. W., Fletterick, R. J., and Craik, C. S. (2004) *J. Biol. Chem.* **279**, 30751–30759
28. Pratje, E., and Guiard, B. (1986) *EMBO J.* **5**, 1313–1317
29. Hahne, K., Haucke, V., Ramage, L., and Schatz, G. (1994) *Cell* **79**, 829–839